OPENMC - APPLICATION ON IAEA CRP – NEUTRONIC BENCHMARK ON CEFR START-UP TESTS

CONTENTS

1. PROJECT: MODELLING A SINGLE FUEL SUB-ASSEMBLY

1.1. WHAT PARTICIPANTS WILL DO IN THIS ACTIVITY?

Here is the list to do during the group activity 2. The OpenMC scratch file for CEFR fuel subassembly is provided. Participants fill the data and simulate the OpenMC.

1. Preprocessing data from 20℃ to 250℃ based on measured information
    - Calculation atomic density for fuels, structural materials, and sodium
    - Calculation the dimension
2. Filling in OpenMC input scratch file
    - Define surfaces that make up fuel subassembly
    - Define pins and lattices in 2D for fuel region
    - Stack universes in 3D
    - Set calculation options: basic options, plotting, and tallies
3. Postprocessing data from OpenMC output
    - All participants get the same k-eff results
    - Visualization the output, such as pin-power distribution, flux spectrum

1.2. WHAT DATA IS NEEDED?

The preparation of the CEFR core input for Monte Carlo simulations will start with collecting and processing the information on the three major components:

1. Operating conditions (primarily operating temperatures). These are needed in order to:
    - Select appropriate temperature dependent XS data or activate correct temperature in a Monte Carlo code;
    - Adjust material compositions and core dimensions due to thermal expansions.
2. Materials
    - List of materials comprising the core (fuel, blanket coolant, control, and structures);
    - Their materials properties including masses, densities, and linear expansion coefficients;
    - Their isotopic compositions.
3. Geometry
    - Axial and radial layouts of all SAs comprising the core;
    - All relevant dimensions at the reference and operating temperatures;
    - Core layout and location of the SAs within the core.

1.3. OPERATING TEMPERATURES

All three experiments, considered in this course, were performed at cold zero power conditions with a target core temperature of **250 °C**. Although the measured core temperatures slightly deviate from this target value, in all simulations the uniform temperature of 250 °C was chosen for all core materials.

1.4. COLLECTING AND PROCESSING OF MATERIAL DATA

According to the benchmark specifications, the CEFR fuel sub-assembly comprises eight unique materials listed in TABLE 1.

TABLE 1. MATERIALS IN THE CEFR CORE

Material	**Used in**	**α_L[†], 1/°C**	**Alias[*]**
Enriched UO_2	Fuel	1.1E-05	UOF
Depleted UO_2	Blanket	1.0E-05	UOB
[+]SS 15-15Ti	Cladding, spacer wires	1.8E-05	1515Ti
[+]SS 316Ti	SS structures not mentioned above	1.8E-05	316Ti
He	Gap	-	He
Sodium	Coolant	See Eq. (25)	Na

[+]SS - stainless steel
[†]α_L - linear expansion coefficient
[*]Alias - material name used in the Monte Carlo input

In order to perform calculations, Monte Carlo codes require nuclide compositions of all materials present in the model. The essential information that should be collected include:

- Total material density (either mass or atomic). Atomic density is often referred to as number density (ND).
- Densities of each nuclide in the material. Both atom fractions and weight fractions can be used.

Care must be taken to assure that the input material densities correspond to actual operating conditions. In case of CEFR, the material and geometry data, provided in the benchmark, corresponds to the installation temperature of 20 °C. To match the operating temperature of 250 °C, material densities should be adjusted using corresponding linear expansion coefficients, α_L according to Eqs. (3) and (4):

$$\varepsilon(T) = \frac{L(T)}{L(T_0)} = 1 + \alpha_L \cdot [T - T_0] \tag{3}$$

$$\rho(T) = \frac{\rho(T_0)}{\varepsilon(T)^3} \tag{4}$$

where T_0 and T are the reference and operating temperatures. L(T), ε(T), and ρ(T) are respectively the temperature dependent linear dimension, linear relative expansion, and mass density. The linear expansion coefficients are shown in TABLE 1. The densities of solid materials will be discussed in the following sub-sections.

1.4.1. Isotopic compositions of fuel and blanket

The isotopic compositions of the fuel and blanket materials were derived from the provided SA-wise total masses of UO_2, U, and U-235 and the known dimensions of the fuel and blanket regions. The SA-wise total masses, provided in the benchmark specifications, were obtained by the averaging the factory certificate data of 89 fabricated fuel SAs. The required data is summarized in TABLE 2 and TABLE 3.

TABLE 2. TOTAL MASSES OF FUEL AND BLANKET COMPONENTS IN A FUEL SA

Component	**Mass, kg/SA**		**Source**
	Fuel	**Blanket**	
UO_2	Get data	Get data	Table 10
U	Get data	Get data	Table 10
U-235	Get data	Get data	Table 10

TABLE 3. DIMENSIONS OF FUEL AND BLANKET REGIONS (AT 20 °C)

Parameter	**Fuel**	**Blanket**	**Source**
Inner pellet radius (r_i), cm	Get data	Get data	FIG. 4
Outer pellet radius (r_o), cm	Get data	Get data	FIG. 4
Total region height (h), cm	Get data	Get data	FIG. 4
Number of fuel pins (n)	Get data	Get data	FIG. 4
Total volume (V), cm^3/SA	Calculate it	Calculate it	Eq. (5)

Total volume, V, of either fuel or blanket regions was calculated using Eq. (5):

$$V = (r_o^2 - r_i^2) \cdot \pi \cdot h \cdot n \tag{5}$$

where r_i is the inner pellet radius, r_o is the outer pellet radius, h is the region height, and n is the total number of fuel rods per SA.

The SA-wise masses and region volumes were farther used to calculate the mass densities of UO_2, U-235, U-238, and O in fuel and blanket regions. For the fuel region the following mass densities were obtained:

$$\rho_{U235} = \frac{m_{U235}}{V} = \frac{get\ data}{calculate\ it} \cdot 1000 \left[\frac{g}{kg}\right] = calculate\ it \left[\frac{g}{cm^3}\right] \tag{6}$$

$$\rho_{U238} = \frac{m_{U238}}{V} = \frac{m_U - m_{U235}}{V} \left[\frac{g}{cm^3}\right] \tag{7}$$

$$\rho_O = \frac{m_O}{V} = \frac{m_{UO2} - m_U}{V} \left[\frac{g}{cm^3}\right] \tag{8}$$

$$\rho_{UO2} = \rho_{U235} + \rho_{U238} + \rho_O \left[\frac{g}{cm^3}\right] \tag{9}$$

Since the obtained material densities correspond to 20 °C, they should be adjusted to match the actual operating temperature of 250 °C using Eqs. (3) and (4), and applying the relevant linear expansion coefficients from TABLE 1.

Please fill the adjusted material densities in TABLE 4 for the fuel and blanket respectively. These data can be directly used in materials, "UOF" and "UOB", in OpenMC input file.

TABLE 4. ISOTOPIC COMPOSITION OF FUEL AND BLANKET

Isotope	Mass density, g/cm^3		ND, #/barn·cm	
	20 ℃	250 ℃	20 ℃	250 ℃
U-235	Calculate it	Calculate it	Calculate it	Calculate it
U-238	Calculate it	Calculate it	Calculate it	Calculate it
O-16[1]	Calculate it	Calculate it	Calculate it	Calculate it
Total	Calculate it	Calculate it	Calculate it	Calculate it

1.4.2. Isotopic compositions of 15-15T and 316T stainless steels

In the CEFR benchmark, the compositions of the 15-15T and 316T SSs are provided as a list of elements with their relative masses, and the total mass density. Although some nuclear data libraries contain XS data for natural elements, it is strongly recommended to decompose them into the isotopic constituents according to the following steps:

1. Obtain atomic masses and natural abundance of all specific isotopes. In the current course the data was taken from The National Institute of Standards and Technology [28].
2. Calculate atomic mass of the elements from isotopic atomic masses and their natural abundances.
3. Calculate the mass density of the elements from total SS mass density and provided relative mass
4. Calculate ND of the elements using the elemental atomic mass and elemental density
5. Calculate ND of specific nuclides from the elemental ND and natural abundance
6. Adjust ND to match operating temperature of 250 °C

Step 2 to 5 are demonstrated using the Fe element in the 316Ti SS as an example:

Step 2 $$A_{Fe} = A_{Fe54} \cdot f_{Fe54} + A_{Fe56} \cdot f_{Fe56} + A_{Fe57} \cdot f_{Fe57} + A_{Fe58} \cdot f_{Fe58}$$

where f is a relative natural abundance.

Step 3 $$\rho_{Fe} = \rho_{316Ti} \cdot w\%_{Fe}$$

where $w\%$ is a relative mass of the element.

Step 4 $$ND_{Fe} = \frac{\rho_{Fe}}{A_{Fe}} \cdot N_{Avo}$$

Step 5 $$ND_{Fe54} = ND_{Fe} \cdot f_{Fe54}$$
$$ND_{Fe56} = ND_{Fe} \cdot f_{Fe56}$$
$$ND_{Fe57} = ND_{Fe} \cdot f_{Fe57}$$
$$ND_{Fe58} = ND_{Fe} \cdot f_{Fe58}$$

Applying the aforementioned procedure will produce the final compositions for the MC calculations. Please get the data and calculate isotopic composition and fill in TABLE 5 for 15-15Ti (SS in OpenMC) and 316Ti (Ti316 in OpenMC) respectively. Relative mass is in Table 12, and atomic masses and natural abundance can be found in [28] (also in Atomic_weights.txt in Jupyter Notebooks).

[1]O-17 and O-18 are neglected due to their low abundance and very minor neutronic importance.

TABLE 5. ISOTOPIC COMPOSITION OF STEEL MATERIALS (15-15TI AND 316 TI)

Element	Relative mass, w%	Isotope	A, g/mol	Natural abundance, %	ND, #/barn·cm	
					20 ℃	250 ℃
Fe	Get data	Fe-54	Get data	Get data	Calculate it	Calculate it
		Fe-56	Get data	Get data	Calculate it	Calculate it
		Fe-57	Get data	Get data	Calculate it	Calculate it
		Fe-58	Get data	Get data	Calculate it	Calculate it
Cr	Get data	Cr-50	Get data	Get data	Calculate it	Calculate it
		Cr-52	Get data	Get data	Calculate it	Calculate it
		Cr-53	Get data	Get data	Calculate it	Calculate it
		Cr-54	Get data	Get data	Calculate it	Calculate it
Ni	Get data	Ni-58	Get data	Get data	Calculate it	Calculate it
		Ni-60	Get data	Get data	Calculate it	Calculate it
		Ni-61	Get data	Get data	Calculate it	Calculate it
		Ni-62	Get data	Get data	Calculate it	Calculate it
		Ni-64	Get data	Get data	Calculate it	Calculate it
Mo	Get data	Mo-92	Get data	Get data	Calculate it	Calculate it
		Mo-94	Get data	Get data	Calculate it	Calculate it
		Mo-95	Get data	Get data	Calculate it	Calculate it
		Mo-96	Get data	Get data	Calculate it	Calculate it
		Mo-97	Get data	Get data	Calculate it	Calculate it
		Mo-98	Get data	Get data	Calculate it	Calculate it
		Mo-100	Get data	Get data	Calculate it	Calculate it
Mn	Get data	Mn-55	Get data	Get data	Calculate it	Calculate it
C	Get data	C-12	Get data	Get data	Calculate it	Calculate it
Ti	Get data	Ti-46	Get data	Get data	Calculate it	Calculate it
		Ti-47	Get data	Get data	Calculate it	Calculate it
		Ti-48	Get data	Get data	Calculate it	Calculate it
		Ti-49	Get data	Get data	Calculate it	Calculate it
		Ti-50	Get data	Get data	Calculate it	Calculate it
Si	Get data	Si-28	Get data	Get data	Calculate it	Calculate it
		Si-29	Get data	Get data	Calculate it	Calculate it
		Si-30	Get data	Get data	Calculate it	Calculate it
				Total:	Calculate it	Calculate it

1.4.3. Material compositions of the sodium coolant

As recommended in the CEFR benchmark specifications [27], the density of liquid sodium can be easily calculated using Eq. (25):

$$\rho_{Na} = 950.0483 - 0.2298\,T - 14.6045 \times 10^{-6}T^2 + 5.6377 \times 10^{-9}T^3 \quad (25)$$

where ρ_{Na} is the sodium density in g/cm^3, and T is the sodium temperature in ℃. Substituting T= 250 ℃ into Eq. (25) will give ρ_{Na} = calculate it g/cm^3. Convert it into the atomic density and fill "Na_FU" in OpenMC input.

1.5. ‘HIERARCHICAL’ APPROACH TO GEOMETRY MODELING

The CEFR core geometry model used in this training course is based on a ‘hierarchical’ approach which tries to follow ‘natural’ core geometry levels. The decomposition of the core model into hierarchical levels facilitates the geometry construction and debugging. As shown in FIG. 1, the CEFR core model comprises 4 hierarchical levels:

— 3D reactor core;
— 3D SAs;
— 2D lattices or cells (X-Y slices of each unique axial region of 3D SAs);
— 2D pins.

The geometry modelling is essentially based on 2 stages:

— Decomposition of the geometry into ‘building’ blocks using the hierarchical levels (i.e. going from the 3D core level to the 2D pin level);
— Defining the building blocks and building the geometry using the ‘inverted’ hierarchical levels (i.e. going from the 2D pin level to the 3D core level).

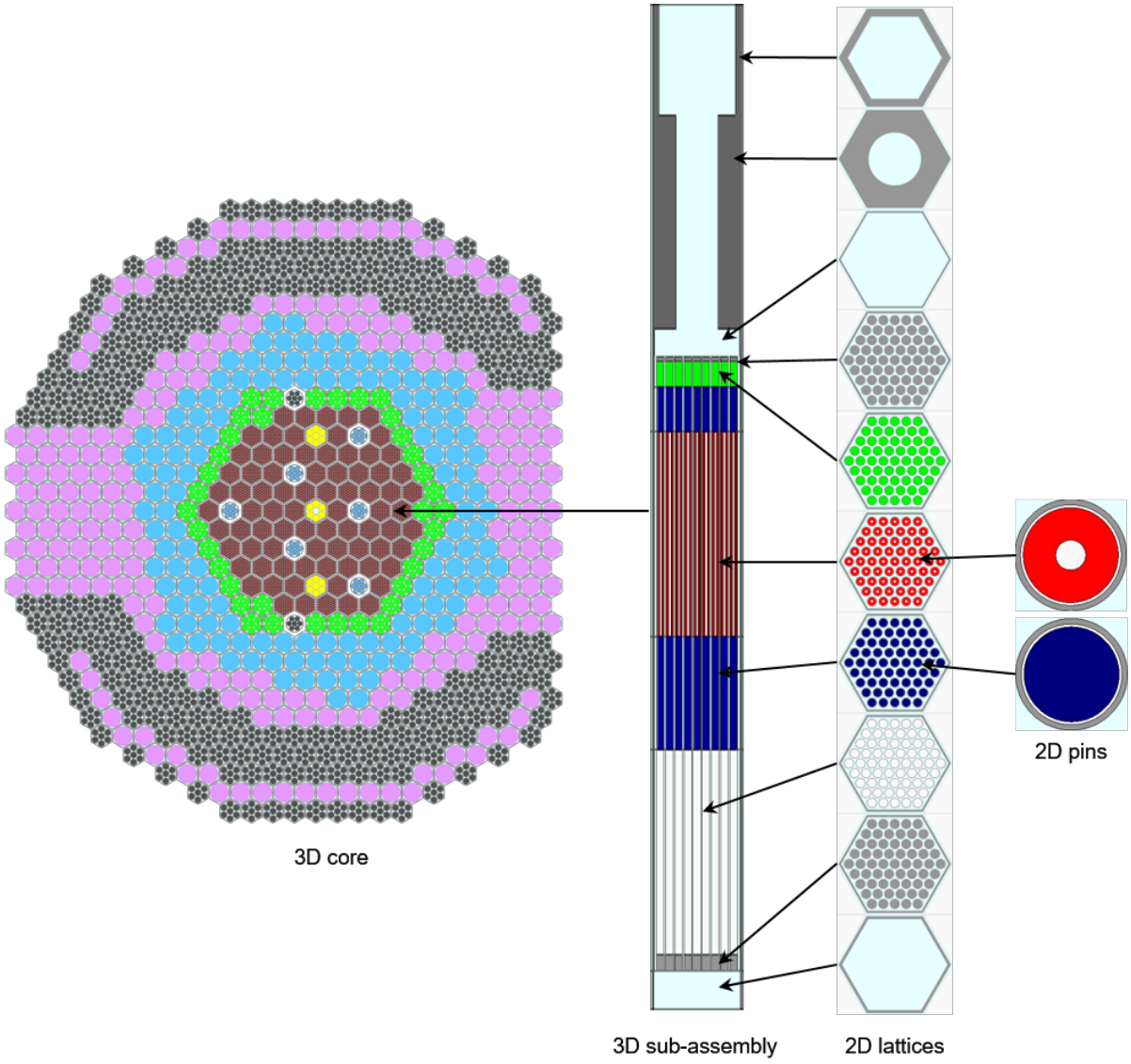

FIG. 1. Hierarchical approach to the CEFR core geometry model based on a fuel sub-assembly

1.5.1. Decomposition of the CEFR core geometry

First, the core containing 712 SAs, is decomposed into eleven 'unique' SA types. However, in this workshop, only fuel SAs should be explicitly defined as separate universes in the MC input.

Second, the SAs are further decomposed into unique heterogeneous axial regions. The constituting axial regions are described in TABLE 6. At this stage, the axial boundaries of each layer should be identified. Next, the axial dimensions are actualized to account for thermal expansions by 1) obtaining the linear relative expansion, ε(T), using linear expansion coefficients from TABLE 1 and Eq. (3); and 2) plugging the obtained ε(T) into Eq. (26)

$$h(T) = \varepsilon(T) \cdot h(T_0) \tag{26}$$

where h is the region height, T_0 = 20 °C, and T = 250 °C.

Finally, the unique axial regions are decomposed, where needed, into unique pins such as fuel or blanket pins in the fuel SA. At this stage, all relevant dimensions should be collected and processed. Please get data from FIG. 4 and calculate axial expanded height of each region.

TABLE 6. DESCRIPTION AND DIMENSIONS OF AXIAL SUB-ASSEMBLY REGIONS

#	a_FU	Upper region boundary at 20 °C, cm	Upper region boundary at 250 °C, cm
1	Head	219.700	220.473
2	Upper shield	196.700	197.377
3	Upper connector	149.700	150.183
4	Top end plug	143.700	144.158
5	Spring	142.700	143.154
6	Upper blanket	Get data	Calculate data
7	Fuel	Get data	Calculate data
8	Lower blanket	Get data	Calculate data
9	Lower gas plenum	57.200	57.437
10	Bottom end plug	12.200	12.251
11	Lower connector	8.700	8.736

1.5.2. Simplifications and approximations

A general approach, adopted in this course, is to model all important regions from neutronic perspective as close as possible to the available specifications, in particular at the active core level. Only peripheral regions, with reduced neutronic importance such as handling heads, are treated in an approximate way, as described in TABLE 7.

TABLE 7. DESCRIPTION OF GEOMETRY-RELATED SIMPLIFICATIONS

Object	Affected region	Simplification
Space wire	Fuel rod	Mixed with cladding
Spring	Fuel rod	Modelled as a homogeneous mixture of steel and He
Supporting plug	Fuel rod	Not modelled
Rounded corners	Fuel pellet	Not modelled
Handling head	Fuel SA	Modelled as hexagonal wrappers of different thickness
Nozzle sector	All SAs	Not modelled.

1.6. OPENMC INPUT DESCRIPTION

This sub-section describes the reference OpenMC input.

1.6.1. Naming convention used in the OpenMC input

The OpenMC model consists of different objects such as materials, surfaces, cells, universes, and lattices. These objects are identified by their names. For example, material names are used to identify the materials in cell cards, surface names are used to identify the surfaces in the cell cards, etc. OpenMC allows to arbitrary choose the name for the objects. To improve readability, the descriptive names were used when possible. The object names were made from compound keywords using underscore (_) character as a separator. Some further details on the adopted naming convention are listed below.

- The surface names start with a short keyword pointing at the surface type;
- The cell names start with "c_" where "c" stands for "cell" (e.g. "c_FU_FIS_0");
- The pin names start with "p_" where "p" stands for "pin" (e.g. "p_FU_FIS");
- The lattices names start with "l_" where "l" stands for "lattice" (e.g. "l_FU_FISS");
- The universe names start with "u_" where "u" stands for "universe" (e.g. "u_FU_FIS");
- The SA names start with "a_" where "a" stands for "assembly" (e.g. "a_FU").

1.6.2. OpenMC input example: building the fuel sub-assembly geometry

Building the geometry using the inverted hierarchical levels (i.e. going from the 2D pin to the 3D SA) is demonstrated on the fuel SA. The rest of the SAs are defined in a similar manner. **The scratch OpenMC input (cefr_tutorial.ipynb) is provided via Jupyter Notebooks, and fill blanks in the file.**

1. Definitions of the surfaces used to construct fuel pins, sub-assemblies.

2. The defined 2D pins are further employed to construct 2D axial regions of the fuel SA including fuel pin lattices mentioned in TABLE 6. (only fuel and blanket regions)

#	2D pin		#	2D pin	
	Content	**Snapshot**		**Content**	**Content**
1	Top end plug	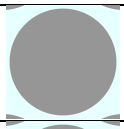	5	Lower blanket	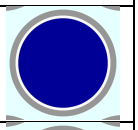
2	Spring	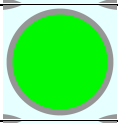	6	Lower gas plenum	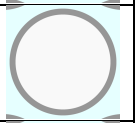
3	Upper blanket	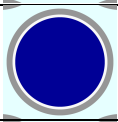	7	Bottom end plug	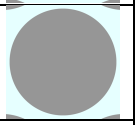
4	Fuel				

FIG. 2. Building 2D pins of the fuel SA regions.

3. The definition of the lattices in 2D and building in 3D fuel subassembly. (only fuel and blanket regions)

#	2D axial region		#	2D axial region	
	Content	Snapshot		Content	Snapshot
0	Outside		6	Upper blanket	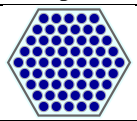
1	Head	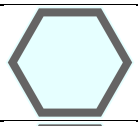	7	Fuel	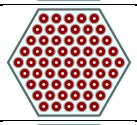
2	Upper shield	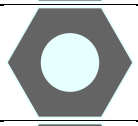	8	Lower blanket	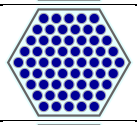
3	Upper connector	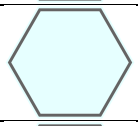	9	Lower gas plenum	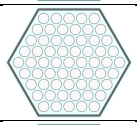
4	Top end plug	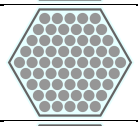	10	Bottom end plug	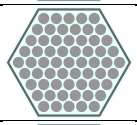
5	Spring	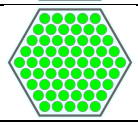	11	Lower connector	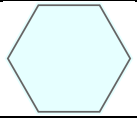

Merge	`a_FU = openmc.Universe()`
	`a_FU.add_cells([c_FU_OUT,c_FU_HEA,c_FU_USH,c_FU_UCN,c_FU_TEP,c_FU_SPR`
	`c_FU_UBL,c_FU_FIS,c_FU_LBL,c_FU_LGP,c_FU_BEP,c_FU_LCN ])`				

FIG. 3. Building 3D fuel SA (a_FU) from 2D axial regions.

2. OPTIONAL ACTIVITIES

The rest of the SAs are defined in a similar manner. Then, it can be expanded this project to modelling a whole core of CEFR to simulate three kinds of simplified benchmarks based on CEFR Start-up Test: first criticality, control rod worth, and sodium void reactivity. Not only rest of a core specifications but also modelling dataset of two Monte Carlo codes (OpenMC and Serpent) are included in "IAEA TCS: Fundamentals of Neutron Simulation of a Fast Reactor Based on IAEA's Benchmark of China Experimental Fast Reactor Start-up Tests." Let's compare your results with those in the TCS.

APPENDIX

DETAILED SPECIFICATION OF CEFR START-UP TEST BENCHMARK

Most of the contents of Appendix I are taken from the Benchmark Specifications in [27].

A.1. GEOMETRY INFORMATION

It should be noted that all the geometric parameters of SAs are based on the installation state, in which all the materials are at a uniform temperature of 20 °C. For other temperatures, the geometric parameters should be recalculated by use of the linear expansion coefficients of each material, listed in TABLE 1. Most of the parameters are given by nominal value or design value, and some of the measured values are provided in specific tables.

Fuel SA

The geometry of fuel SA is shown in attached FIG. 4.

Each fuel SA consists of handling head, upper shielding, hexagonal tube, rod bundle, upper and lower connectors, and nozzle. Fuel SAs are of four types due to the difference in the nozzle structure, which is determined by the power of each SA and specific need for cooling.

In each fuel SA there are 61 fuel rods. The bottom of the rods is held by a set of thin plates, which are welded to the duct, while the top of the rods is free for axial expansion. Radially, the rods are separated by spacer wires.

Both fuel and blanket pellets are cylinders made of sintered UO_2 powder; in each fuel pellet there is a central hole, and the edge is chamfered. Above the pellet stack is the spring, which keeps the pellet stack tight and accommodates its axial elongation due to thermal expansion, swelling and creeping. The pellet stack rest on a small supporting plug made of SS. Below the pellets is the gas plenum to hold the gaseous fission products. The fuel rod is filled with helium gas at a pressure of about 2.6MPa. The rod is sealed by welding the top and bottom end plugs with the cladding.

The design value of pellet density is provided in Table 8, along with some other additional information of fuel pellets. However, in neutronics calculation the smear density is recommended, which is the density of UO_2 if it were uniformly spread or smeared throughout the inside of the cladding. It can be calculated by use of the total mass given in Table 10, which are measured values obtained from the factory certificates of each SA. By use of smear density, there is no need to consider the detailed geometry of fuel or blanket pellets.

TABLE 8. ADDITIONAL INFORMATION OF FUEL ROD

Parameters	Fuel	Blanket
Diameter of pellet [mm]	$5.20^{+0}_{-0.15}$	$5.20^{+0}_{-0.15}$
Diameter of central hole [mm]	1.6±0.1	N/A
Design value of pellet density [g/cm^3]	10.5±0.2	≥10.3
Pressure of helium gas [MPa]	2.6	

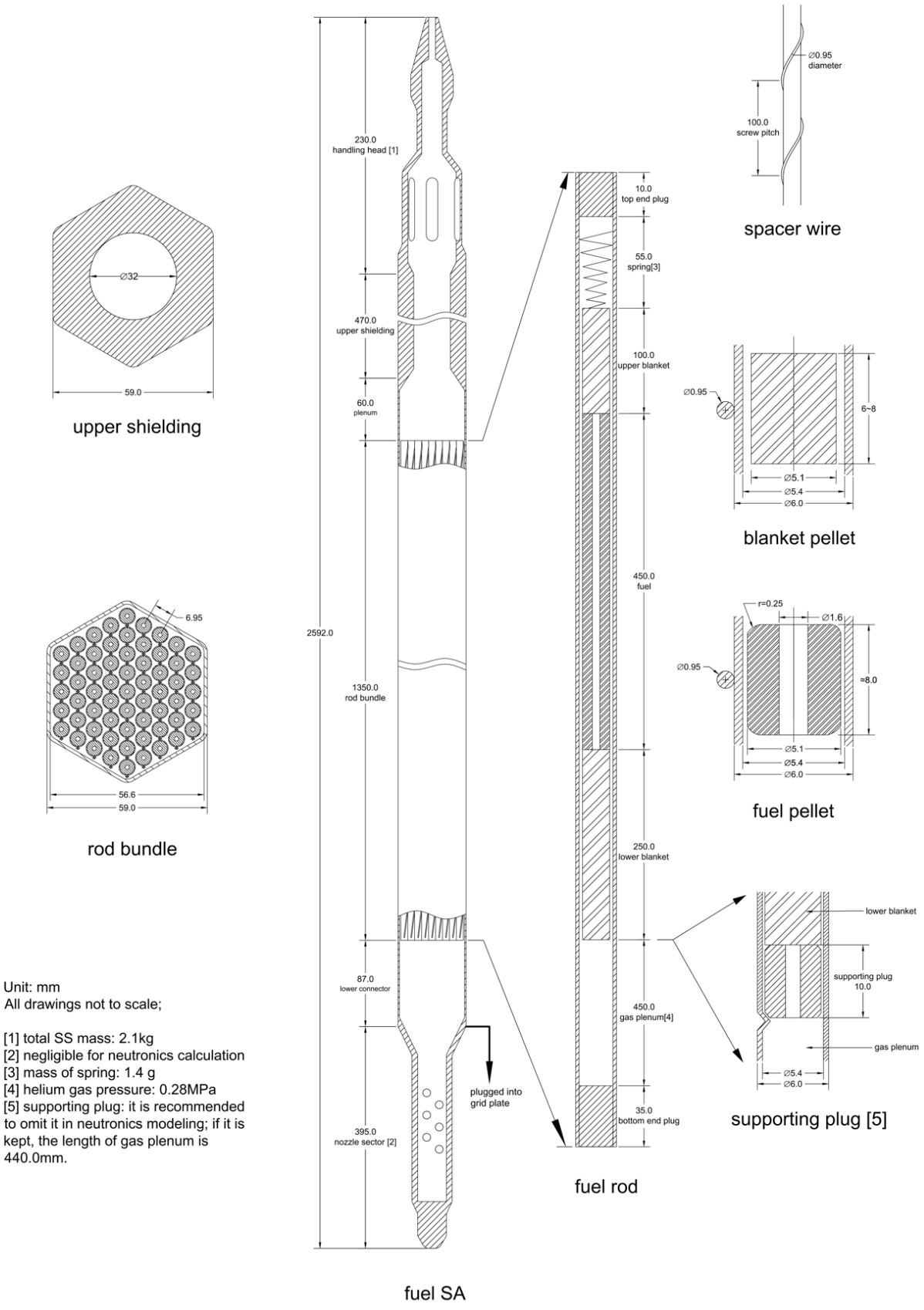
∅32
59.0
upper shielding
6.95
56.6
59.0
rod bundle
Unit: mm
All drawings not to scale;
[1] total SS mass: 2.1kg
[2] negligible for neutronics calculation
[3] mass of spring: 1.4 g
[4] helium gas pressure: 0.28MPa
[5] supporting plug: it is recommended to omit it in neutronics modeling; if it is kept, the length of gas plenum is 440.0mm.
2592.0
230.0
handling head [1]
470.0
upper shielding
60.0
plenum
1350.0
rod bundle
87.0
lower connector
395.0
nozzle sector [2]
plugged into grid plate
fuel SA
10.0
top end plug
55.0
spring[3]
100.0
upper blanket
450.0
fuel
250.0
lower blanket
450.0
gas plenum[4]
35.0
bottom end plug
fuel rod
∅0.95
diameter
100.0
screw pitch
spacer wire
∅0.95
6~8
∅5.1
∅5.4
∅6.0
blanket pellet
r=0.25
Ø1.6
∅0.95
≈8.0
∅5.1
∅5.4
∅6.0
fuel pellet
lower blanket
supporting plug
10.0
gas plenum
∅5.4
∅6.0
supporting plug [5]

FIG. 4. Fuel SA.

A.2. MATERIAL INFORMATION

Fuel and Absorber

TABLE 9. MAIN PARAMETERS OF CORE SUB-ASSEMBLIES*

	Fuel SA	
	Fuel	**Blanket**
Number of SAs in core (operation loading)	79	
Length of SA [mm]	2592	
Mass of SA [kg]	29~31	
Number of rods	61	
Rod lattice pitch [mm]	6.95	
Outer diameter of rod/cladding [mm]	6.00	
Inner diameter of cladding [mm]	5.40	
Diameter of spacer wire [mm]	0.95	
Screw pitch of spacer wire [mm]	100	
Effective material and enrichment	UO_2	
	64.4±0.5 wt%	0.3~0.72 wt%
Total mass of UO_2 or B_4C in each SA [kg]	5.30±0.13	1.28/3.23(1)
Length of effective material [mm]	450	100/250(2)

* All the parameters are given for first loading, at installation temperature of 20 ℃, and in nominal value or design value.
(1): The total mass of UO_2 is 1.28 kg in upper blanket and 3.23 kg in lower blanket of each SA;
(2): The length of upper blanket is 100 mm, and the lower 250 mm.

TABLE 10. TOTAL MASS OF FUEL/BLANKET IN EACH FUEL SA

		Design value	**Measured value**				
			Average	**Standard Deviation**	**Minimum**	**Maximum**	**Total Number***
Fuel	Mass of UO_2 [kg]	5.30±0.13	5.28127	0.01295	5.2570	5.3421	89
	Mass of U [kg]	4.66±0.12	4.64602	0.01167	4.6246	4.6979	
	Mass of ^{235}U [kg]	N/A	2.98197(1)	0.00852	2.9667	3.0156	
	Enrichment of ^{235}U [wt%]	64.4±0.5	64.18315	0.09761	64.08	64.41	
Blanket	Mass of UO_2 [kg]	4.51±0.30	4.56629	0.01548	4.5345	4.6079	
	Mass of U [kg]	3.97±0.28	4.01855	0.01418	3.9940	4.0587	
	Mass of ^{235}U [kg]	N/A	0.0179(1)	3.1403E-04	0.0172	0.0183	
	Enrichment of ^{235}U [wt%]	0.3~0.72	0.44532	0.00719	0.42924	0.45646	

* Totally 89 fuel SAs were manufactured for the first loading, with 10 SAs for backup. The measured value in this table was obtained from the factory certificates of each SA.
(1): This work uses measured average value of ^{235}U in order to get fuel material compositions.

Stainless steel

In the CEFR core, multiple types of SS. are used as structure material, including 15-15Ti, 316Ti, 302, 304, etc. In consideration of both model simplification and precision of neutronics calculation, only two types of SS are kept for the simplified core model, 15-15Ti and 316Ti. The components made of 15-15Ti are listed in Table 11. All the remaining SS components of

are supposed to be made of 316Ti in the simplified core model. The composition of the two SS types is listed in Table 12, in which the density is also listed.

TABLE 11. COMPONENTS MADE OF 15-15TI

SA type	**Components made of 15-15Ti**
Fuel SA	rod cladding, spacer wire
Control SA	rod cladding, spacer wire, cylinder tube (D=49 mm)
Neutron Source SA	central tube (D=20 mm), spacer wire

TABLE 12. COMPOSITION OF STAINLESS STEEL

Element	**Relative Mass [%]**	
	15-15Ti	**316Ti**
C	0.06	0.06
Si	0.45	0.60
Ti	0.35	0.40
V(1)	0.20	0
Cr	16.25	17.00
Mn	1.50	1.75
Fe	64.24	65.19
Ni	14.75	12.50
Mo	2.20	2.50
Density [g/cm^3]	7.97	7.98

(1): This work omits to use V due to lack of cross section library data and negligible contributions.

REFERENCES

[1] BROWN, D. A. et al., ENDF/B-VIII.0: The 8th Major Release of the Nuclear Reaction Data Library with CIELO-project Cross Sections, New Standards and Thermal Scattering Data, Nucl. Data Sheets **148** (2018) 1.

[2] GE, Z., WU, H., CHEN, G., and XU, R., CENDL project, the Chinese evaluated nuclear data library, in EPJ Web of Conferences, (Sept. 2017), **146**, 0200202002.

[3] PLOMPEN, A. J. M. et al., The joint evaluated fission and fusion nuclear data library, JEFF-3.3, European Physical Journal A, **56**. Springer, 1–1081–108, Jul. 14, (2020).

[4] SHIBATA, K. et al., JENDL-4.0: A new library for nuclear science and engineering, J. Nucl. Sci. Technol. **48** (2011) 1.

[5] CONLIN, J. L., KAHLER, A. C., MCCARTNEY, A. P., and REHN, D. A., NJOY21: Next generation nuclear data processing capabilities, EPJ Web Conf. **146** (2017) 09040.

[6] RIMPAULT, G., PLISSON, D., TOMMASI, J., JACQMIN, R., RIEUNIER, J.-M., and DENIS VERRIER, The ERANOS code and data system for fast reactor neutronic analyses, (2002).

[7] LEE, C., JUNG, Y. S., and YANG, W. S., MC2-3: Multigroup Cross Section Generation Code for Fast Reactor Analysis Nuclear Science and Engineering Division, (2018).

[8] RIMPAULT, G. et al., The APOLLO3® Scientific Tool for SFR Neutronic Characterization: Current Achievements and Perspectives, (2017).

[9] FRIDMAN, E. and SHWAGERAUS, E., Modeling of SFR cores with Serpent-DYN3D codes sequence, Ann. Nucl. Energy **53** (2013) 354.

[10] NIKITIN, E., FRIDMAN, E., and MIKITYUK, K., Solution of the OECD/NEA neutronic SFR benchmark with Serpent-DYN3D and Serpent-PARCS code systems, Ann. Nucl. Energy **75** (2015) 492.

[11] NIKITIN, E., FRIDMAN, E., and MIKITYUK, K., On the use of the SPH method in nodal diffusion analyses of SFR cores, Ann. Nucl. Energy **85** (2015) 544.

[12] LEPPÄNEN, J., PUSA, M., VIITANEN, T., VALTAVIRTA, V., and KALTIAISENAHO, T., The Serpent Monte Carlo code: Status, development and applications in 2013, Ann. Nucl. Energy **82** (2015) 142.

[13] ROMANO, P. K., HORELIK, N. E., HERMAN, B. R., NELSON, A. G., FORGET, B., and SMITH, K., OpenMC: A state-of-the-art Monte Carlo code for research and development, Ann. Nucl. Energy **82** (2015).

[14] X-5 MONTE CARLO TEAM, MCNP - A General Monte Carlo N-Particle Transport Code, Version 5, Los Alamos National Laboratory, LA-UR-03-1987, (2003).

[15] SONG, J., WU, Y., and FDS, T., Monte Carlo simulation software super MC 2.2 for fusion and fission applications, in Transactions of the American Nuclear Society,

(2015), **113**.

[16] WANG, K. et al., RMC - A Monte Carlo code for reactor core analysis, Ann. Nucl. Energy **82** (2015).

[17] NAGAYA, Y., OKUMURA, K., and MORI, T., Recent developments of JAEA's Monte Carlo code MVP for reactor physics applications, Ann. Nucl. Energy **82** (2015).

[18] LEE, H. et al., MCS – A Monte Carlo particle transport code for large-scale power reactor analysis, Ann. Nucl. Energy **139** (2020).

[19] SHIM, H. J., HAN, B. S., JONG, S. J., PARK, H. J., and KIM, C. H., McCard: Monte Carlo code for advanced reactor design and analysis, Nucl. Eng. Technol. **44** (2012).

[20] BRUNETT, A. J. and FANNING, T. H., U. S. Sodium Fast Reactor Codes and Methods: Current Capabilities and Path Forward, (2017).

[21] MOHANAKRISHNAN, P., Development and validation of a fast reactor core burnup code - FARCOB, Ann. Nucl. Energy **35** (2008).

[22] WANG, Y., XU, Z., ZHENG, Y., and WU, H., A new hexagonal-Z nodal SN method in SARAX code system, Ann. Nucl. Energy **144** (2020).

[23] DAVIES, U., LINDLEY, B., TOLLIT, B., and SHWAGERAUS, E., Whole-core validation of the Superphenix reactor using WIMS11 and an investigation into a hybrid RZ-HEX SP3 calculation route, (2019).

[24] BATKI, B., PATAKI, I., KERESZTÚRI, A., and PANKA, I., Extension and application of the KIKO3DMG nodal code for fast reactor core analyses, Ann. Nucl. Energy **140** (2020).

[25] DEL-VALLE-GALLEGOS, E., LOPEZ-SOLIS, R., ARRIAGA-RAMIREZ, L., GOMEZ-TORRES, A., and PUENTE-ESPEL, F., Verification of the multi-group diffusion code AZNHEX using the OECD/NEA UAM Sodium Fast Reactor Benchmark, Ann. Nucl. Energy **114** (2018).

[26] NGUYEN, T. D. C., LEE, H., and LEE, D., Use of Monte Carlo code MCS for multigroup cross section generation for fast reactor analysis, Nucl. Eng. Technol. **53** (2021).

[27] HUO, X. et al., Technical Specifications for Neutronics Benchmark of CEFR Start-Up Tests (CRP-I31032), Beijing, China, (2019).

[28] NATIONAL INSTITUTE OF STANDARDS AND TECHNOLOGY, Atomic Weights and Isotopic Compositions for All Elements,. https://physics.nist.gov/cgi-bin/Compositions/stand_alone.pl?ele=&all=all&ascii=ascii

[29] Universe-based geometry type in Serpent - Serpent Wiki,. https://serpent.vtt.fi/mediawiki/index.php/Universe-based_geometry_type_in_Serpent

[30] The OpenMC Monte Carlo Code — OpenMC Documentation,.

https://docs.openmc.org/en/stable/index.html

[31] Surface types - Serpent Wiki,. https://serpent.vtt.fi/mediawiki/index.php/Surface_types